ACS OMEGA

http://pubs.acs.org/journal/acsodf

Article

Phase Equilibrium and Density of CO_2 + Acetic Acid Systems from 308.15 to 338.15 K and 15 to 45 MPa

Teng Zhu, Yuming Li, Houjian Gong,* and Mingzhe Dong

Cite This: *ACS Omega* 2021, 6, 6663−6673

Read Online

ACCESS | Metrics & More | Article Recommendations

ABSTRACT: Using a high-pressure phase equilibrium apparatus and vibrating-tube densimeter, phase transition pressures of CO_2 (1) + acetic acid (2) binary systems with x_2 = 0.000, 0.107, 0.163, 0.222, and 1.000 were measured under temperatures from 308.15 to 338.15 K. Besides, the densities at the same composition and temperature under pressure from 15 to 45 MPa were also detected, and the volumes of mixing (ΔV_m) were calculated. Three prediction models (SRK EOS, PC-SAFT EOS, and TS model) were introduced to predict and correlate the density of binary systems, which was found to have positive relationships with temperature and acetic acid concentration and a negative relationship with pressure. Thereinto, the variation trend of CO_2 density with pressure tends to be flat under high pressure, and which of acetic acid density increased linearly with pressure. ΔV_m are negative, and their absolute value increases with the increase of temperature and the decrease of pressure. The work herein could provide a theoretical guide and basic data for supercritical CO_2 extraction technology and CO_2 application in oil field development.

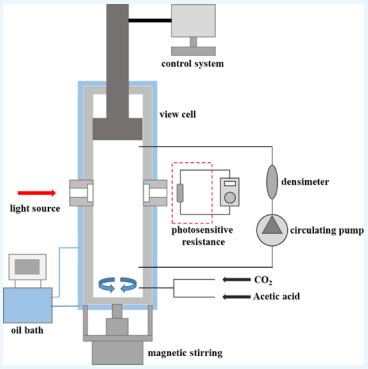

1. INTRODUCTION

Recently, supercritical CO_2 utilization technology in the extraction process has gained much attention.[1,2] It was reported that the transformation of glycerol, as the main byproduct of biodiesel, via the esterification of glycerol and acetic acid could be efficient in high-value downstream product synthesis, such as that of monoglycerate, diglycerate, and triglycerate. During the process, an extra amount of acetic acid residual needs to be extracted to further maximize the resource utilization.[3] The supercritical CO_2 extraction process is an efficient, ecological, stable, and cheap technology that could be used in acetic acid extraction. Thus, the phase behavior and density of CO_2 + acetic acid should be carefully investigated to provide basic data and experimental guide for further application.[4,5]

Moreover, in oil field development, acidification is an efficient route for carbonate reservoir production improvement.[6] However, the general acidification process possesses an excessive reaction rate, leading to well pipe corrosion. The introduction of acetic acid could effectively avoid this situation.[7] At present, supercritical CO_2 fracturing and enhanced oil recovery have already become the hotspots in oil field development. In the deep formation, CO_2 and acetic acid, which have an interaction, could benefit the acidification, fracturing, and enhanced oil recovery processes.[8,9] And it is urgently needed to investigate the phase behavior and density of the CO_2 + acetic acid binary system, which could provide technology support for supercritical CO_2 application in oil field development.

In reported supercritical CO_2 high-pressure phase equilibrium and density measurement methods, visible phase transition pressure measurement and vibrating-tube densimeter measurement, which have the advantage of user-friendly control and nonsampling, have gained much attention.[10,11] The Peng−Robinson (PR) EOS,[12] Soave−Redlich−Kwong (SRK) EOS,[13] and Tait equation[14] are generally used as the equation of state or empirical model of phase transition pressure and density. As reported by Gross et al., the perturbed-chain statistical associating fluid theory equation of state (PC-SAFT EOS) has good prediction for a high-pressure CO_2 system.[15,16] Besides, Toscani and Szwarc reported that a six-parameter empirical model (TS model) could also correlate well with density experimental values under high pressure.[17]

Physically, the accurate determination of phase behavior and thermodynamic properties of a given gas−liquid mixture depends on the α function, binary interaction parameters, mixing rules, and volume translation strategy.[18−21] The original SRK EOS and PR EOS have a relatively large deviation in the prediction of saturated vapor pressure and liquid density. The modification of saturated vapor pressure is carried out by using the α function.[22,23] In principle, the existing α functions can be

Received: November 9, 2020
Accepted: February 25, 2021
Published: March 5, 2021

https://dx.doi.org/10.1021/acsomega.0c05462
ACS Omega 2021, 6, 6663−6673

classified as Soave-type[13,24] and logarithm-type.[25] The Soave-type α function has been found to be the most widely used one for the two-parameter cubic EOSs. However, the traditional Soave-type α function cannot satisfy a basic requirement, that is, it does not exhibit a limiting behavior as the reduced temperature approaches infinity. For this reason, Heyen proposed the logarithmic-type α function.[26] Through the improvement of Trebble and Bishnoi[25] and Twu et al.,[22,27] this kind of α function has been able to solve this problem, and the prediction accuracy has been further improved. Since then, Li and Yang combined the advantages of the two types and obtained a new α function that could better predict the vapor pressure of both pure substance and alkane solvent−CO_2−heavy oil systems.[28] Recently, Chen and Yang optimized the reduced temperature for acentric factor in α function associated with PR EOS and SRK EOS to improve vapor pressure prediction for heavy hydrocarbon compounds.[29] These new α functions can significantly improve the prediction accuracy of phase behavior not only for small molecules but also for complex heavy hydrocarbon components.

At present, the existing cubic EOS can provide reliable prediction for many thermodynamic properties of various substances but cannot give an accurate calculation of liquid volume.[30] To reduce this error, Martin[31] first introduced the concept of volume translation, and Peneloux et al. suggested a constant volume correction in SRK EOS.[32] This method can still be used to evaluate the liquid density in supercritical CO_2[33] and other systems.[34,35] Further research shows that the temperature-dependent volume translation model[36,37] and temperature−volume-dependent volume translation model[38,39] can improve the prediction accuracy. Recently, Chen and Li have fully exploited the potential of the distance function to improve the accuracy of the volume translation SRK EOS in predicting the density of saturated and single-phase liquids.[18]

To predict the density of mixed systems, binary interaction parameters and mixing rules are often used by regression of experimental results.[40] Starting from the original classic van der Waals mixing rule,[12,13] a series of studies of SRK EOS and PR EOS mixed rules, such as the Huron−Vidal mixing rule,[41] MHV2 mixing rule,[42] PHV mixing rule,[43] Wong−Sandler mixing rule,[44] and its modified type.[45] These modified mixing rules and the α function and volume translation we mentioned before make the SRK EOS and PR EOS still have considerable vitality.

To the best of our knowledge, for the CO_2 + acetic acid binary system, the investigation of density under high pressure is still rare.[5] In this work, the combination of a self-designed high-pressure phase equilibrium apparatus with a vibrating-tube densimeter was introduced to detect the phase transition pressures of CO_2 (1) + acetic acid (2) binary with x_2 = 0.107, 0.163, and 0.222, and densities of unitary and binary systems at temperature of 308.15, 318.15, 328.15, and 338.15 K and pressure of 15.00, 20.00, 25.00, 30.00, 35.00, 40.00, and 45.00 MPa. At the same time, the α function, binary interaction parameters, mixing rules, and volume translation strategy are used for accurately determining phase transition pressures and density by using SRK EOS, PR EOS, and PC-SAFT EOS followed by density correlation with the TS model and volume of mixing calculation.

2. MODELING

The phase transition pressure of the CO_2 + acetic acid binary systems was predicted by modifying the α function of SRK EOS and PR EOS. In addition, the SRK EOS, PC-SAFT EOS, and TS model were introduced to predict and correlate the densities of CO_2 + acetic acid unitary and binary systems for experimental reliability validation. And volumes of mixing (ΔV_m) in binary system were also investigated.

2.1. SRK EOS. SRK EOS[13] has the expression of:

$$p = \frac{RT}{V_m - b} - \frac{a}{V_m(V_m + b)} \tag{1}$$

where p, T, and V_m are the pressure, temperature, and molar volume, respectively. R is the ideal gas constant. a and b are parameters.

For pure components, the expressions for a and b are:

$$a_i = \alpha(T_r, \omega) \times 0.42747\frac{R^2 {T_{ci}}^2}{p_{ci}} \tag{2}$$

$$b_i = 0.08664\frac{RT_{ci}}{p_{ci}} \tag{3}$$

where $\alpha(T_r, \omega)$ is the α function, which is dependent upon both the reduced temperature T_r and the acentric factor ω. T_{ci} is the critical temperature, and p_{ci} is the critical pressure. In this paper, the Soave-type α function[13] used in the SRK EOS is given by:

$$\alpha = [1 + (0.48508 + 1.55171\omega - 0.15613\omega^2)(1 - T_r^{0.5})]^2 \tag{4}$$

For mixed systems, a could be decided by adding the standard quadratic mixing term a_0 and asymmetric (polar) term a_1 together.

$$a = a_0 + a_1 \tag{5}$$

Expressions of a_0, a_1, and b are shown below:

$$a_0 = \sum_{i=1}^{n}\sum_{j=1}^{n} x_i x_j (a_i a_j)^{0.5}(1 - \eta_{ij}) \tag{6}$$

$$a_1 = \sum_{i=1}^{n} x_i \left(\sum_{j=1}^{n} x_j ((a_i a_j)^{0.5} l_{ij})^{1/3}\right)^3 \tag{7}$$

$$b = \sum_i x_i b_i \tag{8}$$

In the expressions, x_i is the mole fraction, and η_{ij} and l_{ij} are the binary interaction parameters that could be obtained from density−composition regression. Another three parameters, a_i, a_j, and b_i, are denoted in SRK EOS especially for the pure system.

In this paper, since it is necessary to calculate the density of the liquid phase, the volume translation proposed by Peneloux[32] was used to correct the molar volume:

$$V_m = V_{m0} - c \tag{9}$$

$$c = \sum_{i=1}^{n} x_i c_i \tag{10}$$

https://dx.doi.org/10.1021/acsomega.0c05462
ACS Omega 2021, 6, 6663−6673

Table 1. PC-SAFT EOS Pure-Component Parameters Used in This Work

component	M (g·mol^{-1})	m^{seg}/M (mol·g^{-1})	σ_i (Å)	ε_i (Å)$^{-1}$	$\kappa^{A_iB_i}$	$\varepsilon^{A_iB_i}$ (K)$^{-1}$	ref
CO_2	44.01	0.0471	2.7852	169.21			15
acetic acid	60.05	0.0223	3.8582	211.59	0.07555	3044.4	16

$$c_i = 0.40768\frac{RT_{ci}}{p_{ci}}(0.29411 - Z_{RAi}) \tag{11}$$

where V_{m0} is the molar volume calculated by the equation of state without the correction, c is the Peneloux volume correction term, and c_i is the Peneloux volume correction term for pure components, calculated from the critical temperature (T_{ci}) and pressure (p_{ci}) and the Rackett parameter (Z_{RAi}).

2.2. PR EOS. The expression of the PR EOS[12] is:

$$p = \frac{RT}{V_m - b} - \frac{a}{V_m(V_m + b) + b(V_m - b)} \tag{12}$$

For pure components, the expressions for a and b are:

$$a_i = \alpha(T_r, \omega) \times 0.45724\frac{R^2T_{ci}^{\ 2}}{p_{ci}} \tag{13}$$

$$b_i = 0.077797\frac{RT_{ci}}{p_{ci}} \tag{14}$$

Here, we use the α function modified by Li and Yang[28] to improve phase transition pressure prediction. The expression of this α function used in the PR EOS is given by:

$$\alpha = \exp\{(0.13280 - 0.05052\omega + 0.25948\omega^2)(1 - T_r) + 0.81769\ln[1 + (0.31355 + 1.86745\omega - 0.52604\omega^2)(1 - T_r^{0.5})]^2\} \tag{15}$$

The mixing rule and volume translation are the same as in SRK EOS, and the meanings of each variable in eqs 12 to 15 are the same as those in Section 2.1.

2.3. PC-SAFT EOS. In PC-SAFT EOS,[15,16] compressibility factor (Z) is related to ideal gas ($Z^{id} = 1$), hard-chain (Z^{hc}), segment dispersion (Z^{disp}), and association (Z^{assoc}), which could be expressed as below:

$$Z = 1 + Z^{hc} + Z^{disp} + Z^{assoc} \tag{16}$$

Generally speaking, the non-association molecule could be presented by three parameters from the pure system, which are the number of spheres in the chain (m), the diameter of the spheres (σ), and the segment energy parameter (ε/k). For the association molecule, another two parameters, the effective association volume (κ^{AB}) and the association energy (ε^{AB}), should also be used. For CO_2 and acetic acid used in this work, CO_2, as a non-association molecule, has weak polarity, while acetic acid is an association molecule with strong polarity. The detailed information about these two molecules is listed in Table 1.

For binary system compositing by small molecules, the parameters could be predicted by the conventional Berthelote−Lorentz combining rules,[46] which are shown in the following:

$$\sigma_{ij} = 0.5 \times (\sigma_i + \sigma_j) \tag{17}$$

$$\varepsilon_{ij} = (\varepsilon_i\varepsilon_j)^{0.5}(1 - k_{ij}) \tag{18}$$

$$\varepsilon^{A_iB_j} = 0.5 \times (\varepsilon^{A_iB_i} + \varepsilon^{A_jB_j}) \tag{19}$$

$$\kappa^{A_iB_i} = (\kappa^{A_iB_i} \times \kappa^{A_iB_i})^{0.5} \times \frac{2(\sigma_{ii} \times \sigma_{jj})^{0.5}}{\sigma_{ii} + \sigma_{jj}} \tag{20}$$

Among them, k_{ij} is a binary interaction parameter, as the function of temperature, which could be used to correlate crossing dispersion energy between different molecules. In this work, k_{ij} is obtained by regressing the experimental data of density.

2.4. Toscani−Szwarc (TS) Model. The TS model[17] is an empirical density correlation model with six adjusted parameters, which shows good correlation results in this work. The model could be expressed as below:

$$\rho = \frac{A_1 - A_2T + p + A_3p^{0.5}}{A_4 + A_5p + A_6p^{0.5}} \tag{21}$$

In the model, ρ, p, and T are the mass density in kg·m^{-3}, pressure in MPa, and temperature in K, respectively. A_1−A_6 are the six adjusted parameters, which could be calculated by regressing experimental data.

2.5. Deviation Analysis. Absolute average deviation (AAD), mean deviation (bias), standard deviation (SDV), and root mean square (RMS) are used for deviation analysis between experimental and calculated data. These four deviations could be expressed as follows:[47]

$$\Delta Y_i = \left(\frac{Y_i^{exp} - Y_i^{cal}}{Y_i^{exp}}\right) \tag{22}$$

$$AAD = \frac{1}{n}\sum_{i=1}^{n}|\Delta Y_i| \times 100\% \tag{23}$$

$$Bias = \frac{1}{n}\sum_{i=1}^{n}(\Delta Y_i) \times 100\% \tag{24}$$

$$SDV = \sqrt{\frac{1}{n-1}\sum_{i=1}^{n}(\Delta Y_i - bias)^2} \times 100\% \tag{25}$$

$$RMS = \sqrt{\frac{1}{n}\sum_{i=1}^{n}(\Delta Y_i)^2} \times 100\% \tag{26}$$

Among them, Y_i^{exp} and Y_i^{cal} represent the experimental and calculated value, repectively.

2.6. Volumes of Mixing (ΔV_m). Volumes of mixing (ΔV_m) of the binary system are calculated with the density difference between the mixture and pure chemicals (excess volume), which could be expressed in the following:[48]

$$\Delta V_m = \frac{x_1M_1 + x_2M_2}{\rho} - \frac{x_1M_1}{\rho_1} - \frac{x_2M_2}{\rho_2} \tag{27}$$

https://dx.doi.org/10.1021/acsomega.0c05462
ACS Omega 2021, 6, 6663−6673

In the expression, ΔV_m and ρ are denoted as volumes of mixing and mixture density, respectively. Besides, x_i, M_i, and ρ_i represent the molar fraction, molar weight, and density of the pure system, respectively, with i = 1 as CO_2 and i = 2 as acetic acid.

2.7. Calculation Method. The SRK EOS, PR EOS, PC-SAFT EOS, and TS model were calculated and decided by the commercial software Aspen Plus V11 and MATLAB. All the parameters were correlated with the Marquardt−Levenberg algorithm of least squares optimization.

3. RESULTS AND DISCUSSION

3.1. Phase Transition Pressure. Density measurement has meaning only when the system is homogenous. Thus, herein, the measurement for phase transition pressure was used further for density measurement. The results are listed in Table 2.

Table 2. Phase Transition Pressure for the CO_2 (1) + Acetic Acid (2) Binary System

	p (MPa)			
x_2	T = 308.15 K	T = 318.15 K	T = 328.15 K	T = 338.15 K
0.107	7.14	8.41	9.68	10.92
0.163	6.42	7.70	8.98	10.29
0.222	6.07	7.29	8.50	9.78

The pressure−composition phase diagram of the CO_2 (1) + acetic acid (2) binary system could be found in Figure 1. In this figure, solid dots stand for the experimental data, red lines represent the SRK EOS calculation results with η_{ij} = 0.024 and l_{ij} = 0 using the Soave-type α function, and black lines express the PR EOS calculation results with η_{ij} = 0 and l_{ij} = 0 using the α function modified by Li and Yang. It clearly shows that PR EOS has a better ability in phase transition pressure prediction compared with that of SRK EOS. The AAD values of PR EOS and SRK EOS are 3.72 and 5.31%, respectively, indicating that the modified α function can better predict the results of phase transition pressure of the CO_2 + acetic acid binary system.

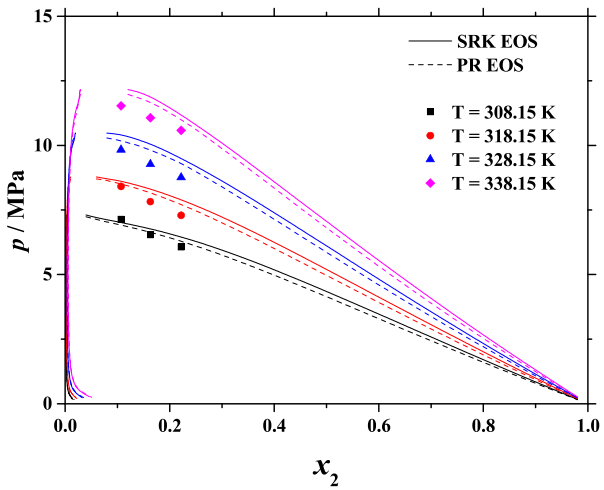

Figure 1. Experimental data (solid dot) and calculation ones (solid lines for SRK EOS and dash lines for PR EOS) of the CO_2 (1) + acetic acid (2) binary system. The black, red, blue, and magenta dots and lines represent temperatures of 308.15, 318.15, 328.15, and 338.15 K, respectively.

The phase transition pressure, which is only used for further density measurement under high pressure, would not be discussed further in this work.

3.2. Density. In this work, the SRK EOS, PR EOS, PC-SAFT EOS, and TS model were used to calculate the density of CO_2 + ethyl acetate systems comparing with the experimental results. Among them, the AAD values of SRK EOS and PR EOS are about the same. To save space, only the calculation results using SRK EOS, PC-SAFT EOS, and TS models are presented in the following paper.

3.2.1. Experimental Results. Density measurement results for CO_2, acetic acid, and CO_2 (1) + acetic acid (2) systems are listed in Table 3. It could be found that the densities for all the systems have a positive relationship with pressure and negative relationship with temperature. The density of CO_2 is more affected by temperature and pressure than that of acetic acid. In detail, the density variation for CO_2 would flatten under high pressure. That is, under low pressure (≤15 MPa), the CO_2 molecules are easy to be compressed. As the pressure is boosted, the difficulty of compression for CO_2 also increases. These correspond with the gas characteristics under high pressure.[11,49] Besides, the density of acetic acid is found to

Table 3. Experimental Data for the Densities of CO_2 (1) + Acetic Acid (2) Systems[a]

	ρ (kg·m^{-3})				
p (MPa)	x_2 = 0.000	x_2 = 0.107	x_2 = 0.163	x_2 = 0.222	x_2 = 1.000
			T = 308.15 K		
15.00	806	914	950	978	1058
20.00	853	944	974	997	1066
25.00	890	969	994	1013	1073
30.00	920	990	1012	1028	1080
35.00	944	1009	1028	1042	1086
40.00	965	1025	1042	1055	1092
45.00	989	1041	1055	1066	1098
			T = 318.15 K		
15.00	730	866	911	945	1049
20.00	804	903	939	967	1057
25.00	845	932	962	986	1064
30.00	879	956	982	1003	1071
35.00	909	978	1000	1018	1078
40.00	934	996	1016	1032	1084
45.00	957	1013	1031	1044	1090
			T = 328.15 K		
15.00	648	817	869	909	1039
20.00	743	858	902	935	1047
25.00	800	893	929	957	1055
30.00	835	922	952	976	1062
35.00	873	946	972	993	1069
40.00	899	967	990	1008	1076
45.00	928	985	1006	1022	1082
			T = 338.15 K		
15.00	557	762	827	872	1030
20.00	679	811	863	902	1038
25.00	749	853	894	927	1046
30.00	799	885	920	948	1053
35.00	839	913	943	967	1061
40.00	867	936	962	984	1067
45.00	897	957	980	999	1074

[a]Uncertainty: $u(T)$ = 0.05 K, $u(p)$ = 0.02 MPa, and $u(\rho)$ = 4.6 kg·m^{-3}.

https://dx.doi.org/10.1021/acsomega.0c05462
ACS Omega 2021, 6, 6663−6673

Table 4. Adjusted Parameters for the TS Models for Densities of CO_2 (1) + Acetic Acid (2) Systems

	values				
parameters	x_2 = 0.000	x_2 = 0.107	x_2 = 0.163	x_2 = 0.222	x_2 = 1.000
A_1 (MPa)	1.163×10^6	67.97	86.16	128.5	107.6
A_2 (MPa·K^{-1})	1.273×10^4	0.1902	0.2176	0.3302	0.07561
A_3 (MPa$^{0.5}$)	1.034×10^6	2.592	4.161	12.84	−3.899
A_4 (MPa·m^3·kg^{-1})	−3432	0.01177	0.02232	0.02982	0.0812
A_5 (m^3·kg^{-1})	−49.8	0.0006575	0.0006347	0.0004251	0.0008208
A_6 (MPa$^{0.5}$·m^3·kg^{-1})	1476	0.004117	0.005413	0.01477	−0.003613

have a positive linear relationship with pressure, which is similar with the characteristic of liquids, such as water and ethanol.[50−52]

3.2.2. Calculation Results and Deviation Analysis. SRK-EOS and PC-SAFT EOS were used to predict the density of CO_2 + acetic acid unitary and binary systems, and the TS model was also introduced for correlation. All the adjusted parameters of the TS model are listed in Table 4. The calculation results and deviation analysis of four statistical values—AAD, bias, SDV, and RMS—from different models are presented in Table 5. Comparison of density−pressure curves obtained from calculation with experimental data is shown in Figure 2. For clarity, only prediction curves calculated from SRK-EOS with n_{ij} = 0.024 and l_{ij} = 0 and from PC-SAFT EOS with k_{ij} = 0.061 are used herein for comparison.

From Table 5 and Figure 2, it could be illustrated that SRK EOS and PC-SAFT EOS have good integral prediction ability for unitary and binary systems, with overall AAD of 1.75 and 0.92%, respectively. Between them, SRK EOS has a relatively larger prediction deviation for unitary system, although the Peneloux volume correction has been used, with AAD for pure CO_2 and pure acetic acid of 2.92 and 5.26%, respectively, which might be caused by the simplicity of its expressions. For pure CO_2 and pure acetic acid systems, SRK EOS and PC-SAFT EOS have greater prediction deviation at higher temperature and lower pressure, while for binary systems, the prediction accuracy of the two equations of state is the highest at medium pressure (30 MPa). On the whole, the prediction accuracy of two kinds of EOS for the binary system is obviously better than that of the unitary system. It should be noticed here that the TS model, as a simple model with six adjusted parameters, could correlate well with experimental results of density under high pressure, which has an AAD value of only 0.10%.

3.2.3. Calculation of ΔV_m. Volumes of mixing (ΔV_m) could be used to evaluate the deviation between mixture and ideal state. In this work, eq 17 was used to calculate the ΔV_m of the CO_2 (1) + acetic acid (2) system with x_2 = 0.107, 0.163, and 0.222, and the results are listed in Table 6. It can be clearly seen that all the ΔV_m under the conditions used herein are negative. This might be caused by the formation of Lewis acid−base interaction between CO_2 and acetic acid.[53,54] With strong affinity between CO_2 and carbonyl of acetic acid, CO_2 molecules could easily insert into the gap between acetic acid molecules and thus cause negative values of ΔV_m.[55]

By comparison of the ΔV_m under different temperatures and pressures, the absolute values of ΔV_m were found to increase with temperature increase or pressure release. This might be caused by the lower density of the mixture system and bigger intermolecular space at relative high temperature (338.15 K) and low pressure (15 MPa), leading to the increase of absolute value of ΔV_m.[56]

4. CONCLUSIONS

A high-pressure phase equilibrium apparatus was introduced to measure the transition phase pressure of CO_2 (1) + acetic acid (2) at 308.15−338.15 K, and PR EOS was found to have a better prediction ability in transition phase pressure than SRK EOS by the modified α function. Besides, a vibrating-tube densimeter was used for CO_2 (1) + acetic acid (2) density measurement with x_2 = 0.000, 0.107, 0.163, 0.222, and 1.000 at 308.15−338.15 K and 15−45 MPa. By calculation of ΔV_m, the SRK EOS, PC-SAFT EOS, and TS model were applied to predict and correlate the density results.

The densities of all systems were found to have positive relationships with temperature and acetic acid concentration but a negative relationship with pressure. Therein, the CO_2 density would flatten under high pressure, which is in accordance with the characteristics of gases under high pressure generally reported. The SRK EOS, PC-SAFT EOS, and TS model have good prediction and correlation performance for densities of pure CO_2, pure acetic acid, and CO_2 + acetic acid binary systems, with AAD values of 1.75, 0.92, and 0.10%, respectively. The ΔV_m are all negative values, and their absolute values increased with temperature increase or pressure decrease. This might be caused by the Lewis acid−base relationship formation between CO_2 and carbonyl of acetic acid.

All the experimental and calculation data obtained herein could provide a theoretical guide and data foundation for supercritical CO_2 utilization in extraction and oil field exploration.

5. EXPERIMENTAL SECTION

5.1. Chemicals. All chemicals used in this work are listed in Table 7 and are not further purified.

5.2. Structure of the High-Pressure Phase Equilibrium Apparatus. The visible and volume-variable high-pressure phase equilibrium apparatus was used to measure the phase behavior and density of CO_2 and acetic acid systems. The apparatus was built by Jiangsu Haian Oilfield Scientific Instrument Co., Ltd., and modified somewhat by our group to satisfy the demand for density measurement under high pressure. The detailed composition and operation method of this supercritical CO_2 phase equilibrium device, which is shown in Figure 3, have been described in our previous works.[57,58]

A brief introduction would be given here. The apparatus is composed of a supercharging device (including piston pump, piston cylinder, etc.), high-pressure visible unit (including high-pressure autoclave, sapphire window, servo motor controller, etc.), temperature and pressure control system

https://dx.doi.org/10.1021/acsomega.0c05462
ACS Omega 2021, 6, 6663−6673

Table 5. Calculated Results and Deviation Analysis of Density of the CO_2 (1) + Acetic Acid (2) System[a]

	x_2 = 0.000					
	SRK EOS		PC-SAFT EOS		TS model	
p (MPa)	ρ_{cal} (kg·m^{-3})	$\Delta Y_i \times 100$	ρ_{cal} (kg·m^{-3})	$\Delta Y_i \times 100$	ρ_{cal} (kg·m^{-3})	$\Delta Y_i \times 100$
			T = 308.15 K			
15.00	750	6.95	797	1.12	810	−0.50
20.00	820	3.87	851	0.23	858	−0.59
25.00	870	2.25	889	0.12	892	−0.22
30.00	910	1.09	918	0.22	919	0.11
35.00	943	0.11	943	0.11	944	0.04
40.00	971	−0.62	965	0.02	966	−0.10
45.00	996	−0.71	983	0.61	988	0.12
			T = 318.15 K			
15.00	670	8.22	716	1.92	727	0.41
20.00	760	5.47	792	1.49	799	0.62
25.00	820	2.96	840	0.59	845	−0.03
30.00	865	1.59	876	0.34	879	0.04
35.00	902	0.77	905	0.44	908	0.11
40.00	934	0.04	929	0.54	934	0.00
45.00	961	−0.42	951	0.63	958	−0.11
			T = 328.15 K			
15.00	583	10.03	621	4.17	644	0.62
20.00	697	6.19	728	2.02	741	0.27
25.00	767	4.13	788	1.50	798	0.25
30.00	820	1.80	832	0.36	839	−0.48
35.00	861	1.37	865	0.92	872	0.11
40.00	896	0.33	893	0.67	901	−0.22
45.00	926	0.22	917	1.19	928	0.03
			T = 338.15 K			
15.00	534	4.13	523	6.10	561	−0.72
20.00	633	6.77	660	2.80	682	−0.44
25.00	715	4.54	735	1.87	750	−0.13
30.00	774	3.13	786	1.63	798	0.13
35.00	820	2.26	825	1.67	837	0.24
40.00	858	1.04	857	1.15	869	−0.23
45.00	891	0.67	884	1.45	897	0.03
AAD (%)		2.92		1.27		0.25
bias (%)		−2.80		−1.27		0.03
SDV (%)		3.02		1.37		0.33
RMS (%)		3.77		1.71		0.31

	x_2 = 0.107					
	SRK EOS		PC-SAFT EOS		TS model	
p (MPa)	ρ_{cal} (kg·m^{-3})	$\Delta Y_i \times 100$	ρ_{cal} (kg·m^{-3})	$\Delta Y_i \times 100$	ρ_{cal} (kg·m^{-3})	$\Delta Y_i \times 100$
			T = 308.15 K			
15.00	909	0.55	917	−0.33	915	−0.13
20.00	940	0.42	944	−0.03	945	−0.11
25.00	967	0.21	966	0.31	970	−0.08
30.00	990	0.02	985	0.51	991	−0.10
35.00	1010	−0.12	1001	0.79	1009	0.02
40.00	1028	−0.29	1017	0.78	1026	−0.11
45.00	1044	−0.29	1030	1.06	1040	0.10
			T = 318.15 K			
15.00	861	0.58	872	−0.69	865	0.12
20.00	899	0.44	905	−0.22	901	0.22
25.00	929	0.32	931	0.11	931	0.12
30.00	955	0.10	953	0.31	956	0.00
35.00	978	−0.01	972	0.61	977	0.10
40.00	998	−0.20	989	0.70	996	−0.04
45.00	1016	−0.30	1004	0.89	1013	−0.01
			T = 328.15 K			
15.00	810	0.86	823	−0.73	814	0.37
20.00	855	0.35	863	−0.58	857	0.12
25.00	890	0.34	894	−0.11	892	0.11
30.00	920	0.22	920	0.22	921	0.15
35.00	945	0.11	942	0.42	945	0.12
40.00	968	−0.10	961	0.62	966	0.10
45.00	987	−0.20	978	0.71	985	0.01
			T = 338.15 K			
15.00	754	1.05	770	−1.05	764	−0.26
20.00	809	0.25	817	−0.74	813	−0.25
25.00	850	0.35	855	−0.23	853	−0.01
30.00	884	0.11	885	0.02	885	0.02
35.00	912	0.13	910	0.33	913	0.01
40.00	937	−0.11	932	0.43	937	−0.11
45.00	958	−0.10	951	0.63	957	−0.03
AAD (%)		0.28		0.96		0.10
bias (%)		−0.16		0.29		−0.01
SDV (%)		0.34		2.38		0.13
RMS(%)		0.35		2.24		0.12

	x_2 = 0.163					
	SRK EOS		PC-SAFT EOS		TS model	
p (MPa)	ρ_{cal} (kg·m^{-3})	$\Delta Y_i \times 100$	ρ_{cal} (kg·m^{-3})	$\Delta Y_i \times 100$	ρ_{cal} (kg·m^{-3})	$\Delta Y_i \times 100$
			T = 308.15 K			
15.00	951	−0.11	952	−0.21	951	−0.11
20.00	975	−0.10	973	0.10	975	−0.10
25.00	996	−0.20	991	0.30	995	−0.07
30.00	1014	−0.20	1007	0.49	1013	−0.13
35.00	1030	−0.19	1021	0.68	1028	0.01
40.00	1045	−0.29	1034	0.77	1042	0.03
45.00	1059	−0.38	1047	0.76	1055	−0.03
			T = 318.15 K			
15.00	912	−0.11	916	−0.55	910	0.11
20.00	940	−0.11	941	−0.21	938	0.11
25.00	963	−0.10	962	0.01	961	0.10
30.00	984	−0.20	980	0.20	982	0.00
35.00	1002	−0.20	996	0.40	1000	0.02
40.00	1018	−0.20	1010	0.59	1016	−0.00
45.00	1033	−0.19	1024	0.68	1030	0.10
			T = 328.15 K			
15.00	870	−0.12	876	−0.81	869	0.03
20.00	902	0.01	906	−0.44	901	0.14
25.00	929	0.00	930	−0.11	928	0.13
30.00	952	−0.00	951	0.12	951	0.11
35.00	973	−0.11	969	0.31	971	0.10
40.00	991	−0.12	985	0.51	989	0.07
45.00	1007	−0.08	1000	0.60	1005	0.11
			T = 338.15 K			
15.00	826	0.12	833	−0.73	827	0.01
20.00	863	0.04	869	−0.72	864	−0.12
25.00	894	0.02	898	−0.45	895	−0.11
30.00	920	−0.04	921	−0.11	921	−0.11
35.00	943	−0.03	942	0.11	943	0.03
40.00	963	−0.12	960	0.21	963	−0.11

https://dx.doi.org/10.1021/acsomega.0c05462
ACS Omega 2021, 6, 6663−6673

Table 5. continued

x_2 = 0.163						
	SRK EOS		PC-SAFT EOS		TS model	
p (MPa)	ρ_{cal} (kg·m^{-3})	$\Delta Y_i \times 100$	ρ_{cal} (kg·m^{-3})	$\Delta Y_i \times 100$	ρ_{cal} (kg·m^{-3})	$\Delta Y_i \times 100$
T = 338.15 K						
45.00	981	−0.11	976	0.41	980	0.04
AAD (%)		0.13		0.50		0.06
bias (%)		0.12		−0.02		0.00
SDV (%)		0.11		0.76		0.08
RMS (%)		0.15		0.71		0.07

x_2 = 0.222						
	SRK EOS		PC-SAFT EOS		TS model	
p (MPa)	ρ_{cal} (kg·m^{-3})	$\Delta Y_i \times 100$	ρ_{cal} (kg·m^{-3})	$\Delta Y_i \times 100$	ρ_{cal} (kg·m^{-3})	$\Delta Y_i \times 100$
T = 308.15 K						
15.00	981	−0.31	978	0.03	979	−0.10
20.00	1000	−0.33	995	0.22	998	−0.10
25.00	1016	−0.32	1011	0.21	1014	−0.11
30.00	1031	−0.29	1024	0.39	1029	−0.13
35.00	1044	−0.19	1037	0.48	1043	−0.12
40.00	1057	−0.19	1048	0.66	1055	0.04
45.00	1068	−0.19	1059	0.66	1067	−0.09
T = 318.15 K						
15.00	948	−0.32	948	−0.32	944	0.11
20.00	969	−0.21	968	−0.10	966	0.12
25.00	988	−0.22	985	0.12	986	−0.01
30.00	1004	−0.11	1000	0.31	1002	0.11
35.00	1019	−0.14	1014	0.39	1018	−0.03
40.00	1033	−0.13	1027	0.48	1031	0.11
45.00	1045	−0.12	1039	0.48	1044	0.02
T = 328.15 K						
15.00	913	−0.44	916	−0.77	909	0.03
20.00	937	−0.21	939	−0.43	935	0.01
25.00	958	−0.10	958	−0.10	957	−0.02
30.00	977	−0.10	976	0.02	976	−0.04
35.00	993	0.03	991	0.20	993	0.03
40.00	1008	0.01	1005	0.33	1008	0.01
45.00	1022	−0.03	1018	0.39	1022	−0.01
T = 338.15 K						
15.00	876	−0.46	881	−1.03	873	−0.13
20.00	904	−0.22	908	−0.67	903	−0.11
25.00	927	−0.02	930	−0.32	928	−0.13
30.00	948	−0.00	950	−0.21	949	−0.11
35.00	967	0.01	967	−0.03	968	−0.10
40.00	983	0.11	982	0.22	984	0.02
45.00	998	0.10	996	0.30	1000	−0.10
AAD (%)		0.16		0.35		0.06
bias (%)		0.15		−0.07		0.03
SDV (%)		0.15		0.42		0.07
RMS (%)		0.19		0.40		0.07

x_2 = 1.000						
	SRK EOS		PC-SAFT EOS		TS model	
p (MPa)	ρ_{cal} (kg·m^{-3})	$\Delta Y_i \times 100$	ρ_{cal} (kg·m^{-3})	$\Delta Y_i \times 100$	ρ_{cal} (kg·m^{-3})	$\Delta Y_i \times 100$
T = 308.15 K						
15.00	1011	4.44	1040	1.70	1059	−0.10
20.00	1015	4.78	1048	1.69	1066	−0.03
25.00	1019	5.03	1055	1.68	1074	−0.09
30.00	1023	5.28	1061	1.76	1080	0.02
35.00	1026	5.52	1068	1.66	1087	−0.07
40.00	1030	5.68	1074	1.65	1093	−0.09
45.00	1033	5.92	1080	1.64	1098	0.01
T = 318.15 K						
15.00	1000	4.67	1032	1.62	1049	0.03
20.00	1005	4.92	1040	1.61	1057	0.02
25.00	1009	5.17	1047	1.60	1064	0.02
30.00	1013	5.42	1054	1.59	1072	−0.09
35.00	1017	5.66	1060	1.67	1078	−0.04
40.00	1020	5.900.	1067	1.57	1084	−0.03
45.00	1024	6.06	1073	1.56	1090	−0.01
T = 328.15 K						
15.00	989	4.81	1024	1.44	1040	−0.12
20.00	994	5.06	1032	1.43	1048	−0.13
25.00	998	5.4	1039	1.52	1055	−0.04
30.00	1003	5.56	1046	1.51	1063	−0.09
35.00	1007	5.8	1053	1.50	1070	−0.09
40.00	1011	6.04	1060	1.49	1076	0.03
45.00	1014	6.28	1066	1.48	1082	0.02
T = 338.15 K						
15.00	978	5.05	1016	1.36	1030	0.01
20.00	983	5.30	1024	1.35	1039	−0.11
25.00	987	5.64	1031	1.43	1046	−0.04
30.00	992	5.79	1039	1.33	1054	−0.09
35.00	996	6.13	1046	1.41	1061	0.03
40.00	1001	6.19	1052	1.41	1068	−0.09
45.00	1005	6.42	1059	1.40	1074	0.01
AAD (%)		5.26		1.54		0.05
bias (%)		−5.26		−1.54		0.05
SDV (%)		1.90		0.53		0.03
RMS (%)		5.05		1.47		0.05

Overall			
	SRK EOS	PC-SAFT EOS	TS model
AAD (%)	1.75	0.92	0.10
bias (%)	−1.59	−0.52	0.02
SDV (%)	1.10	1.09	0.13
RMS (%)	1.90	1.31	0.12

[a]Uncertainty: $u(T)$ = 0.05 K, $u(p)$ = 0.02 MPa, and $u(\rho)$ = 4.6 kg·m^{-3}.

(including oil bath, temperature sensor, pressure sensor, etc.), phase equilibrium measurement unit (including photosensitive resistance, light source, etc.), and density measurement unit.

Gas could be supercharged through the piston pump and piston cylinder that are not shown in Figure 1. With the servo motor to control the piston, the volume and pressure of visible unit could be varied. The temperature of visible unit was adjusted by the oil bath. The deviation caused by observation could be minimized with the introduction of photosensitive resistance that could vary accompanied by system turbidity.

https://dx.doi.org/10.1021/acsomega.0c05462
ACS Omega 2021, 6, 6663−6673

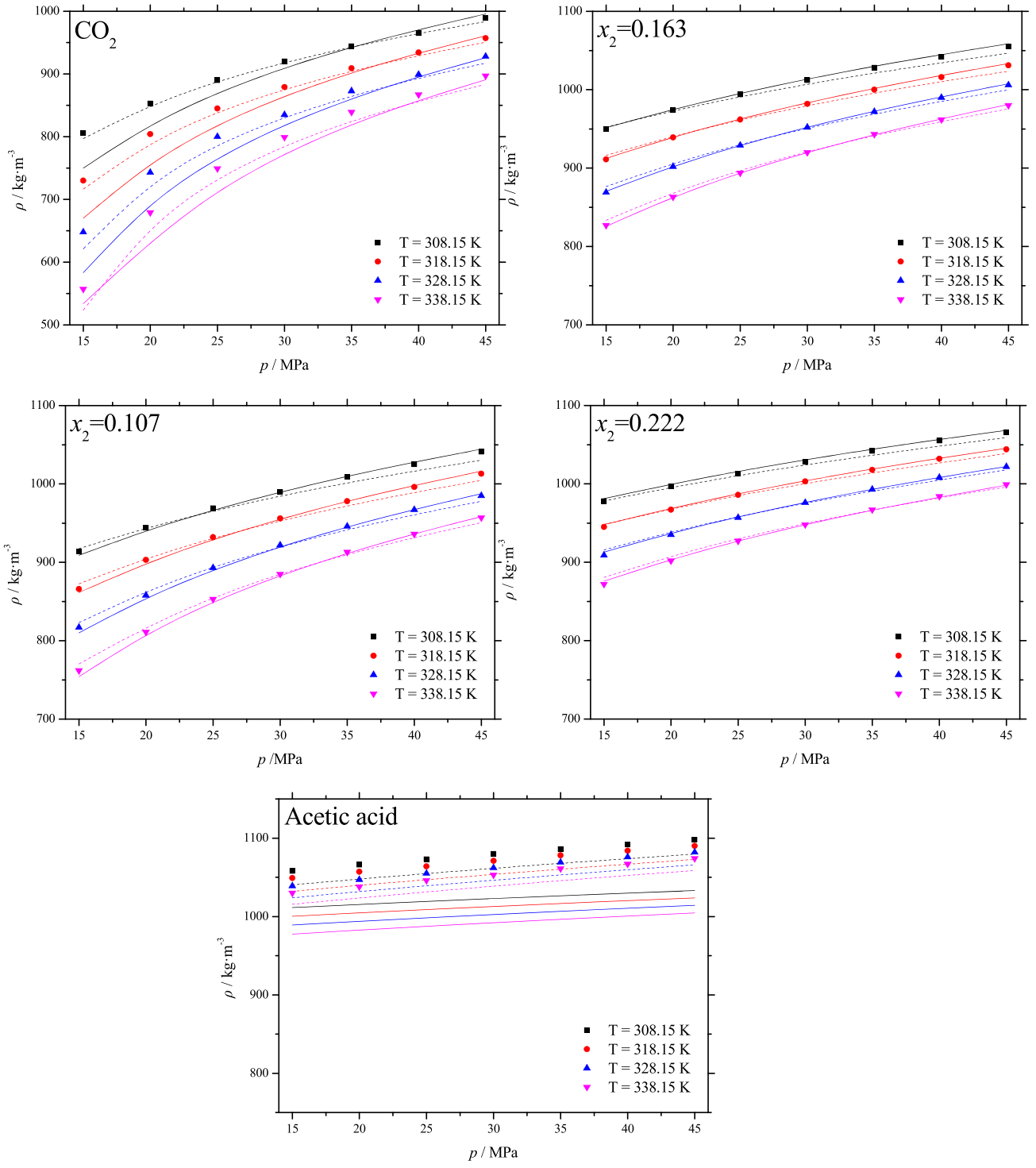

Figure 2. Density−pressure curves of CO_2 (1) + acetic acid (2) unitary and binary systems. Symbols represent experimental data from this work. Solid and dash lines represent the density calculated using the SRK EOS and PC-SAFT EOS, respectively. The black, red, blue, and magenta dots and lines represent temperatures of 308.15, 318.15, 328.15, and 338.15 K, respectively.

The density measurement unit includes a vibrating-tube densimeter and evaluation unit (DMA^{TM} HPM and mPDS-5, provided by Anton Paar Co., Ltd.), a pressure sensor, a temperature detector, a computer, and a circulating pump. The vibrating-tube densimeter is a U-shaped pipe made of Hastelloy C-276 alloy. The density of as-detected fluid could be thus decided by the relationship between oscillation period and mass of vibrating tube.

The phase equilibrium device and density measurement unit can bear a maximum temperature of 423 K and maximum pressure of 50 MPa. The uncertainties of temperature, pressure, and density measurement are ±0.05 K, ±0.02 MPa, and 4.6 kg·m^{-3}, respectively.

5.3. Method for Phase Equilibrium and Density Measurement. The measurement method for phase transition pressure and density of the CO_2 + acetic acid system is listed herein. First of all, a certain amount of acetic acid was

https://dx.doi.org/10.1021/acsomega.0c05462
ACS Omega 2021, 6, 6663−6673

Table 6. ΔV_m ($cm^3 \cdot mol^{-1}$) for CO_2 (1) + Acetic Acid (2) Binary Systems at Different Temperatures and Pressures

	ΔV_m ($cm^3 \cdot mol^{-1}$)		
p (MPa)	x_2 = 0.107	x_2 = 0.163	x_2 = 0.222
	T = 308.15 K		
15.00	−4.805	−5.876	−6.440
20.00	−3.662	−4.498	−4.932
25.00	−2.957	−3.605	−3.935
30.00	−2.480	−3.031	−3.286
35.00	−2.230	−2.680	−2.893
40.00	−1.999	−2.391	−2.599
45.00	−1.665	−1.967	−2.136
	T = 318.15 K		
15.00	−7.160	−8.612	−9.273
20.00	−4.322	−5.423	−6.005
25.00	−3.486	−4.326	−4.803
30.00	−2.880	−3.567	−3.972
35.00	−2.441	−2.979	−3.304
40.00	−2.096	−2.579	−2.862
45.00	−1.822	−2.249	−2.443
	T = 328.15 K		
15.00	−10.865	−12.614	−13.337
20.00	−5.738	−7.236	−7.938
25.00	−4.011	−5.135	−5.728
30.00	−3.523	−4.357	−4.818
35.00	−2.692	−3.384	−3.785
40.00	−2.401	−2.976	−3.283
45.00	−1.866	−2.394	−2.670
	T = 338.15 K		
15.00	−16.788	−19.259	−19.861
20.00	−7.688	−9.655	−10.531
25.00	−5.008	−6.386	−7.142
30.00	−3.621	−4.720	−5.333
35.00	−2.815	−3.688	−4.181
40.00	−2.499	−3.194	−3.642
45.00	−2.016	−2.604	−2.966

Table 7. Specifications of Pure Components

reagent	CAS number	supplier	mass fraction	purification	analysis method
CO_2	124-38-9	Qingdao Tianyuan Gas Co., Ltd.	>0.9999	none	GC[a]
acetic acid	64-19-7	Guangdong Xilong Chemical Co., Ltd.	>0.998	none	GC[a]

[a]Gas chromatography.

added into the visible unit followed by high-pressure CO_2 that was introduced by a supercharging device. The mass of CO_2 in the visible device could be detected by the balance. After temperature setting, the pressure of as-detected fluid was modulated. When the system became bright and homogenous, the pressure at the moment was just higher than that of its phase transition point. Subsequently, the pressure was released until phase separation occurred. The pressure of the phase transition point could be exactly confirmed by the variation of photosensitive resistance.

After the end of phase transition pressure measurement, the circulating pump was opened to transport the fluid through the vibrating-tube densimeter. Instantaneous density under different temperature and pressure could be measured by the

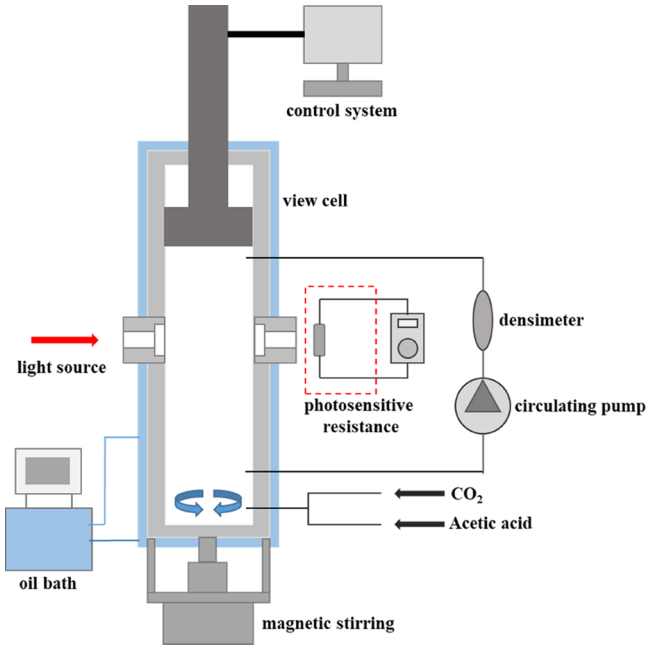

Figure 3. Schematic diagram of the high-pressure phase equilibrium apparatus.

mPDS-5 unit accompanied by a computer to evaluate and detect.

5.4. Comparison with Results in the Reference. Experimental data regarding the investigation of a CO_2 + acetic acid system under high pressure are very rare; thus, only the density of the pure CO_2 system would be compared herein. From Figure 4, it could be found that the deviation of

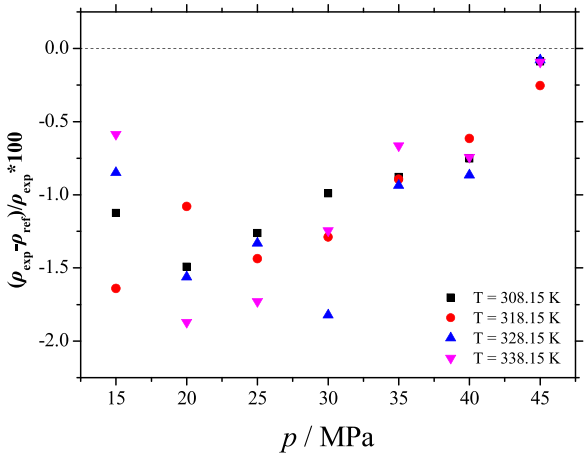

Figure 4. Relative deviations of comparison of density for the pure CO_2 system between measured data in this work and reference values.[59] [Reproduced in part from ref 51. Copyright 2020 American Chemical Society]

experimental data and the ones in the reference[59] is small with an absolute average deviation (AAD) of 1.80%, which indicates the reliability of this work.

5.5. Establishment of Experimental Conditions. This work was based on the density and phase behavior investigation by mixing a large amount of CO_2 with a little acetic acid. Here, 0.107, 0.163, and 0.222 of acetic acid molar fraction were chosen. The temperature was controlled at

https://dx.doi.org/10.1021/acsomega.0c05462
ACS Omega 2021, 6, 6663−6673

308.15, 318.15, 328.15, and 338.15 K. Meanwhile, it would have significance for density measurement provided that the pressure is higher than the miscibility pressure. Thus, pressure was set as 15.00, 20.00, 25.00, 30.00, 35.00, 40.00, and 45.00 MPa.

AUTHOR INFORMATION

Corresponding Author

Houjian Gong − *School of Petroleum Engineering, China University of Petroleum (East China), Qingdao, Shandong 266580, PR China;* orcid.org/0000-0002-3304-1605; Email: gonghoujian@upc.edu.cn

Authors

Teng Zhu − *State Key Laboratory of Heavy Oil Processing, College of Science, China University of Petroleum, Beijing 102249, PR China*

Yuming Li − *State Key Laboratory of Heavy Oil Processing, China University of Petroleum, Beijing 102249, PR China*

Mingzhe Dong − *Department of Chemical and Petroleum Engineering, University of Calgary, Calgary, Alberta, Canada T2N 1N4*

Complete contact information is available at: https://pubs.acs.org/10.1021/acsomega.0c05462

Notes

The authors declare no competing financial interest.

ACKNOWLEDGMENTS

We gratefully acknowledge the financial support from the Natural Science Foundation of Shandong Province of China (ZR2019MEE058), National Natural Science Foundation of China (21802167), and Scientific Research Foundation of China University of Petroleum (Beijing) (ZX20180164).

REFERENCES

(1) Hosseini, S. R. P.; Tavakoli, O.; Sarrafzadeh, M. H. Experimental optimization of SC-CO_2 extraction of carotenoids from *Dunaliella salina*. *J. Supercrit. Fluids* **2017**, *121*, 89−95.

(2) Baldino, L.; Adami, R.; Reverchon, E. Concentration of *Ruta graveolens* active compounds using SC-CO_2extraction coupled with fractional separation. *J. Supercrit. Fluids* **2018**, *131*, 82−86.

(3) Ghaziaskar, H. S.; Afsari, S.; Rezayat, M.; Rastegari, H. Quaternary solubility of acetic acid, diacetin and triacetin in supercritical carbon dioxide. *J. Supercrit. Fluids* **2017**, *119*, 52−57.

(4) Byun, H.-S.; Kim, K.; McHugh, M. A. Phase behavior and modeling of supercritical carbon dioxide− organic acid mixtures. *Ind. Eng. Chem. Res.* **2000**, *39*, 4580−4587.

(5) Bamberger, A.; Sieder, G.; Maurer, G. High-pressure (vapor + liquid) equilibrium in binary mixtures of (carbon dioxide + water or acetic acid) at temperatures from 313 to 353 K. *J. Supercrit. Fluids* **2000**, *17*, 97−110.

(6) Shi, Y.; Yu, L.; Chen, S.; He, Y.; Yang, X.; Duan, L.; Cai, J. Effects of L-glutamic acid, N, N-diacetic acid as chelating agent on acidification of carbonate reservoirs in acidic environments. *J. Nat. Gas Sci. Eng.* **2020**, *82*, 103494.

(7) Yang, L.; Xu, T.; Wei, M.; Feng, G.; Wang, F.; Wang, K. Dissolution of arkose in dilute acetic acid solution under conditions relevant to burial diagenesis. *Appl. Geochem.* **2015**, *54*, 65−73.

(8) Jin, L.; Hawthorne, S.; Sorensen, J.; Pekot, L.; Kurz, B.; Smith, S.; Heebink, L.; Herdegen, V.; Bosshart, N.; Torres, J.; Dalkhaa, C.; Peterson, K.; Gorecki, C.; Steadman, E.; Harju, J. Advancing CO_2 enhanced oil recovery and storage in unconventional oil play—experimental studies on Bakken shales. *Appl. Energy* **2017**, *208*, 171−183.

(9) Middleton, R. S.; Carey, J. W.; Currier, R. P.; Hyman, J. D.; Kang, Q.; Karra, S.; Jiménez-Martínez, J.; Porter, M. L.; Viswanathan, H. S. Shale gas and non-aqueous fracturing fluids: Opportunities and challenges for supercritical CO_2. *Appl. Energy* **2015**, *147*, 500−509.

(10) Li, X.; Han, H.; Yang, D.; Liu, X.; Qin, J. Phase behavior of C_3H_8−CO_2−heavy oil systems in the presence of aqueous phase under reservoir conditions. *Fuel* **2017**, *209*, 358−370.

(11) Gomez-Osorio, M. A.; Browne, R. A.; Carvajal Diaz, M.; Hall, K. R.; Holste, J. C. Density measurements for ethane, carbon dioxide, and methane + nitrogen mixtures from 300 to 470 K up to 137 MPa using a vibrating tube densimeter. *J. Chem. Eng. Data* **2016**, *61*, 2791−2798.

(12) Peng, D.-Y.; Robinson, D. B. A new two-constant equation of state. *Ind. Eng. Chem. Fundamen.* **1976**, *15*, 59−64.

(13) Soave, G. Equilibrium constants from a modified Redlich-Kwong equation of state. *Chem. Eng. Sci.* **1972**, *27*, 1197−1203.

(14) Dymond, J. H.; Malhotra, R. The Tait equation: 100 years on. *Int. J. Thermophys.* **1988**, *9*, 941−951.

(15) Gross, J.; Sadowski, G. Perturbed-chain SAFT: An equation of state based on a perturbation theory for chain molecules. *Ind. Eng. Chem. Res.* **2001**, *40*, 1244−1260.

(16) Gross, J.; Sadowski, G. Application of the perturbed-chain SAFT equation of state to associating systems. *Ind. Eng. Chem. Res.* **2002**, *41*, 5510−5515.

(17) Toscani, S.; Szwarc, H. Two empirical equations of state for liquids to improve *p*, *V*, *T*data representation and physical meaning. *J. Chem. Eng. Data* **2004**, *49*, 163−172.

(18) Chen, X.; Li, H. An improved volume-translated SRK EOS dedicated to more accurate determination of saturated and single-phase liquid densities. *Fluid Phase Equilib.* **2020**, *521*, 112724.

(19) Chen, Z.; Yang, D. A tangent-line approach for effective density used in ideal mixing rule: part I—prediction of density for heavy-oil/bitumen associated systems. *SPE J.* **2020**, *25*, 1,140−1,1154.

(20) Chen, Z.; Yang, D. A tangent-line approach for effective density used in the ideal mixing rule: part II—evaluation of mixing characteristics of oil/gas systems and application criteria. *SPE J.* **2020**, *25*, 3160−3185.

(21) Li, X.; Yang, D.; Zhang, X.; Zhang, G.; Gao, J. Binary interaction parameters of CO_2-heavy-*n*-alkanes systems by using Peng−Robinson equation of state with modified alpha function. *Fluid Phase Equilib.* **2016**, *417*, 77−86.

(22) Twu, C. H.; Coon, J. E.; Cunningham, J. R. A new generalized alpha function for a cubic equation of state Part 2. Redlich-Kwong equation. *Fluid Phase Equilib.* **1995**, *105*, 61−69.

(23) Privat, R.; Visconte, M.; Zazoua-Khames, A.; Jaubert, J.-N.; Gani, R. Analysis and prediction of the alpha-function parameters used in cubic equations of state. *Chem. Eng. Sci.* **2015**, *126*, 584−603.

(24) Robinson, D. B.; Peng, D.-Y. *The characterization of the heptanes and heavier fractions for the GPA Peng-Robinson programs*; Gas processors association: 1978.

(25) Trebble, M. A.; Bishnoi, P. R. Development of a new four-parameter cubic equation of state. *Fluid Phase Equilib.* **1987**, *35*, 1−18.

(26) Heyen, G. *Proceedings of the 2nd World Congress of Chemical Engineering*; Montreal, QC, Canada, 1981, 41−46.

(27) Twu, C. H.; Coon, J. E.; Cunningham, J. R. A new generalized alpha function for a cubic equation of state Part 1. Peng-Robinson equation. *Fluid Phase Equilib.* **1995**, *105*, 49−59.

(28) Li, H.; Yang, D. Modified α function for the Peng− Robinson equation of state to improve the vapor pressure prediction of non-hydrocarbon and hydrocarbon compounds. *Energy Fuel* **2011**, *25*, 215−223.

(29) Chen, Z.; Yang, D. Optimization of the Reduced Temperature Associated With Peng−Robinson Equation of State and Soave−Redlich−Kwong Equation of State to Improve Vapor Pressure Prediction for Heavy Hydrocarbon Compounds. *J. Chem. Eng. Data* **2017**, *62*, 3488−3500.

(30) Pina-Martinez, A.; Le Guennec, Y.; Privat, R.; Jaubert, J.-N.; Mathias, P. M. Analysis of the combinations of property data that are

suitable for a safe estimation of consistent Twu α-function parameters: updated parameter values for the translated-consistent *tc*-PR and *tc*-RK cubic equations of state. *J. Chem. Eng. Data* **2018**, *63*, 3980−3988.
(31) Martin, J. J. Cubic equations of state-which? *Ind. Eng. Chem. Fundamen.* **1979**, *18*, 81−97.
(32) Péneloux, A.; Rauzy, E.; Fréze, R. A consistent correction for Redlich-Kwong-Soave volumes. *Fluid Phase Equilib.* **1982**, *8*, 7−23.
(33) Cardoso, S. G.; Costa, G. M.; de Melo, S. A. B. V. Assessment of the liquid mixture density effect on the prediction of supercritical carbon dioxide volume expansion of organic solvents by Peng-Robinson equation of state. *Fluid Phase Equilib.* **2016**, *425*, 196−205.
(34) Bell, I. H.; Welliquet, J.; Mondejar, M. E.; Bazyleva, A.; Quoilin, S.; Haglind, F. Application of the group contribution volume translated Peng−Robinson equation of state to new commercial refrigerant mixtures. *Int. J. Refrig.* **2019**, *103*, 316−328.
(35) Sun, T.; Takbiri-Borujeni, A.; Nourozieh, H.; Gu, M. Application of Peng-Robinson equation of state for modelling the multiphase equilibrium properties in Athabasca bitumen/ethane mixtures. *Fuel* **2019**, *252*, 439−447.
(36) Shi, J.; Li, H. A.; Pang, W. An improved volume translation strategy for PR EOS without crossover issue. *Fluid Phase Equilib.* **2018**, *470*, 164−175.
(37) Baled, H.; Enick, R. M.; Wu, Y.; McHugh, M. A.; Burgess, W.; Tapriyal, D.; Morreale, B. D. Prediction of hydrocarbon densities at extreme conditions using volume-translated SRK and PR equations of state fit to high temperature, high pressure *PVT* data. *Fluid Phase Equilib.* **2012**, *317*, 65−76.
(38) Abudour, A. M.; Mohammad, S. A.; Robinson, R. L., Jr.; Gasem, K. A. Volume-translated Peng-Robinson equation of state for liquid densities of diverse binary mixtures. *Fluid Phase Equilib.* **2013**, *349*, 37−55.
(39) Frey, K.; Modell, M.; Tester, J. W. Density-and-temperature-dependent volume translation for the SRK EOS: 2. Mixtures. *Fluid Phase Equilib.* **2013**, *343*, 13−23.
(40) Soave, G.; Gamba, S.; Pellegrini, L. A. SRK equation of state: Predicting binary interaction parameters of hydrocarbons and related compounds. *Fluid Phase Equilib.* **2010**, *299*, 285−293.
(41) Huron, M.-J.; Vidal, J. New mixing rules in simple equations of state for representing vapour-liquid equilibria of strongly non-ideal mixtures. *Fluid Phase Equilib.* **1979**, *3*, 255−271.
(42) Michelsen, M. L. A method for incorporating excess Gibbs energy models in equations of state. *Fluid Phase Equilib.* **1990**, *60*, 47−58.
(43) Holderbaum, T.; Gmehling, J. PSRK: A group contribution equation of state based on UNIFAC. *Fluid Phase Equilib.* **1991**, *70*, 251−265.
(44) Wong, D. S. H.; Sandler, S. I. A theoretically correct mixing rule for cubic equations of state. *AIChE J.* **1992**, *38*, 671−680.
(45) Thakre, N.; Jana, A. K. Modeling phase equilibrium with a modified Wong-Sandler mixing rule for natural gas hydrates: Experimental validation. *Appl. Energy* **2017**, *205*, 749−760.
(46) Delhommelle, J.; Millié, P. Inadequacy of the Lorentz-Berthelot combining rules for accurate predictions of equilibrium properties by molecular simulation. *Mol. Phys.* **2001**, *99*, 619−625.
(47) Zúñiga-Moreno, A.; Galicia-Luna, L. A.; Betancourt-Cárdenas, F. F. Compressed liquid densities and excess volumes of CO_2 + thiophene binary mixtures from 313 to 363 K and pressures up to 25 MPa. *Fluid Phase Equilib.* **2005**, *236*, 193−204.
(48) Liu, Q.; Zhao, L.; Zheng, Q.; Mou, L.; Zhang, P. Excess molar volume and viscosity deviation of $[C_2mim][NTf_2]/[C_4mim][NTf_2]$ + DMC/DEC. *J. Chem. Eng. Data* **2018**, *63*, 4484−4496.
(49) Kato, M.; Kokubo, M.; Ohashi, K.; Sato, A.; Kodama, D. Correlation of high pressure density behaviors for fluid mixtures made of carbon dioxide with solvent at 313.15 K. *Open Thermodyn. J.* **2009**, *3*, 1−6.
(50) Weiss, L.; Tazibt, A.; Tidu, A.; Aillerie, M. Water density and polarizability deduced from the refractive index determined by interferometric measurements up to 250 MPa. *J. Chem. Phys.* **2012**, *136*, 124201.
(51) Zhu, T.; Gong, H.; Dong, M. Density and viscosity of CO_2 + ethanol binary systems measured by a capillary viscometer from 308.15 to 338.15 K and 15 to 45 MPa. *J. Chem. Eng. Data* **2020**, *65*, 3820−3833.
(52) Seifried, B.; Temelli, F. Density of carbon dioxide expanded ethanol at (313.2, 328.2, and 343.2) K. *J. Chem. Eng. Data* **2010**, *55*, 2410−2415.
(53) Liu, K.; Kiran, E. Viscosity, density and excess volume of acetone+ carbon dioxide mixtures at high pressures. *Ind. Eng. Chem. Res.* **2007**, *46*, 5453−5462.
(54) Zarei, H.; Golroudbari, S. A.; Behroozi, M. Experimental studies on volumetric and viscometric properties of binary and ternary mixtures of *N*,*N*-dimethylacetamide, *N*-methylformamide and propane-1, 2-diol at different temperatures. *J. Mol. Liq.* **2013**, *187*, 260−265.
(55) Yang, C.; Lai, H.; Liu, Z.; Ma, P. Densities and viscosities of diethyl carbonate+ toluene,+ methanol, and+ 2-propanol from (293.15 to 363.15) K. *J. Chem. Eng. Data* **2006**, *51*, 584−589.
(56) Henni, A.; Hromek, J. J.; Tontiwachwuthikul, P.; Chakma, A. Volumetric properties and viscosities for aqueous AMP solutions from 25 °C to 70 °C. *J. Chem. Eng. Data* **2003**, *48*, 551−556.
(57) Zhu, T.; Gong, H.; Dong, M.; Yang, Z.; Guo, C.; Liu, M. Phase behavior for poly (vinylacetate) + carbon dioxide + cosolvent ternary systems. *J. Chem. Eng. Data* **2017**, *63*, 187−196.
(58) Zhu, T.; Gong, H.; Dong, M.; Yang, Z.; Guo, C.; Liu, M. Phase equilibrium of PVAc + CO_2 binary systems and PVAc + CO_2 + ethanol ternary systems. *Fluid Phase Equilib.* **2018**, *458*, 264−271.
(59) Span, R.; Wagner, W. A new equation of state for carbon dioxide covering the fluid region from the triple-point temperature to 1100 K at pressures up to 800 MPa. *J. Phys. Chem. Ref. Data* **1996**, *25*, 1509−1596.

https://dx.doi.org/10.1021/acsomega.0c05462
ACS Omega 2021, 6, 6663−6673